Conf-9405128--1
SAND94-0934C

DISCLAIMER

D-D FUSION EXPERIMENTS USING FAST Z PINCHES*

R. B. Spielman, G. T. Baldwin, G. Cooper,† D. Hebron, T. W. Hussey,§
C. Landron, R. J. Leeper, S. F. Lopez, J. S. McGurn, D. J. Muron,
J. L. Porter, L. Ruggles, C. L. Ruiz, A. Schmidlapp, and M. Vargas
Sandia National Laboratories
Albuquerque, NM 87185

INTRODUCTION

The development of high current (I > 10 MA) drivers provides us with a new tool for the study of neutron-producing plasmas in the thermal regime. The imploded deuterium mass (or collisionality) increases as I^2 and the ability of the driver to heat the plasma to relevant fusion temperatures improves as the power of the driver increases. Additionally, fast (< 100 ns) implosions are more stable to the usual MHD instabilities that plagued the traditional slower implosions.

We describe experiments in which deuterium gas puffs or CD_2 fiber arrays were imploded in a fast z-pinch configuration on Sandia's Saturn facility generating up to $3X10^{12}$ D-D neutrons. These experiments were designed to explore the physics of neutron-generating plasmas in a z-pinch geometry. Specifically, we intended to produce neutrons from a nearly thermal plasma where the electrons and ions have a nearly Maxwellian distribution. This is to be clearly differentiated from the more usual D-D beam-target neutrons generated in many dense plasma focus (DPF) devices.

EXPERIMENTAL DESCRIPTION

These experiments were conducted on the Saturn accelerator at Sandia National Laboratories, Albuquerque, New Mexico. Saturn is a 25-TW electrical driver capable of delivering up to 10 MA in 40 ns to a z-pinch load. The pulsed power details of the Saturn accelerator have been previously described in detail.[1-3]

The z-pinch load consisted of either an annular, deuterium gas puff or an array of deuterated polyethylene fibers. Some shots were annular gas-puff shots with a single, deuterated-polyethylene fiber on axis. The gas-puff load was produced using a supersonic nozzle. The effective Mach number of the nozzle is ~ Mach 6. The outer diameters of the annular nozzles were either 4.5 cm or 3.5 cm. The thickness of the gas-puff annulus was 1.0 cm. The nozzle was tilted inward at 5 degrees to generate a more uniform pinch by

*This work supported by the U.S. Department of Energy under Contract DE-AC04-76-DP00789.
† Permanent Address: University of New Mexico, Albuquerque, NM 87131.
§ Present Address: Phillips Laboratory, Albuquerque, NM 87185

eliminating the zippering phenomenon.[4] The pinch length was defined using a highly transparent mesh of 125-μm-diameter nickel wire. The length of the pinches used in these experiments was 2 cm. Machine timing is determined by using a breakdown pin, biased at -700 V, placed just upstream of the nozzle throat. Typical delays of 750 μs were used between the breakdown pin signal and the firing of the machine to allow the gas flow to reach nearly steady state. The deuterium gas was always preionized using VUV flash board sources. More details on the operation of Saturn with gas puff z pinches are found in Ref. 5. A schematic of the gas puff load arrangement is shown in Fig. 1. The deuterated-polyethylene fiber array had 48, 25-μm diameter fibers and was 1.5 cm in diameter and 2-cm long. The wires were coated with 1-2 μm of conducting carbon for more uniform breakdown.

In the gas puff experiments, the deuterium gas pressure was varied to adjust the implosion velocity (the specific energy per ion) over the range of 40-100 cm/μs. This impacts, in a self consistent way, the peak plasma temperature and peak plasma density. For higher velocity, lower mass implosions the deuterium plasma attains a higher peak temperature but at the expense of a lower peak density. This will be discussed in greater detail in the Theory Section.

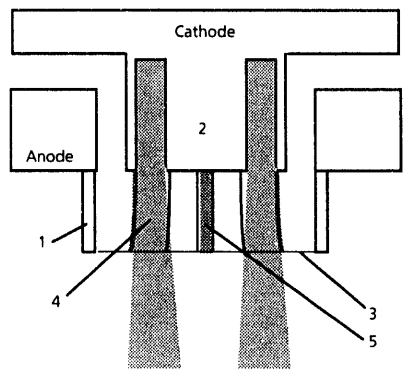

Figure 1 A schematic of the deuterium gas-puff z-pinch load configuration showing the anode and cathode electrodes, the anode current return posts (1), the supersonic gas nozzle (2), the current return wires (3), the initial position of the injected gas (4), and the final pinch (5).

DIAGNOSTICS

These experiments used a array of both x-ray and neutron diagnostics to study the plasma conditions. The x-ray diagnostics were used to obtain indications of pinch performance; final pinch diameter, electron temperature, stagnation and thermalization time, and implosion velocity. Time-integrated and time-resolved x-ray pinhole cameras, filtered with 25.4 μm of beryllium, looked at the x-ray emission above 1 keV. X-ray photoconducting detectors[6] (PCDs) were used to obtain time histories of the keV x-ray pulses in various coarse spectral bands above 1 keV. We had resistive bolometers[7] to measure the total x-ray yields from the pinch. All of the x-ray diagnostics were placed on radial lines-of-sight at an angle of 55 degrees off the pinch axis. Additional x-ray detector information can be found in Ref. 8.

We used a number of neutron diagnostics to measure the fusion performance of the pinch. Absolute measurement of the D-D neutron yields were obtained through indium activation. In this diagnostic, five pure-indium samples each weighing 5.5 g were placed near

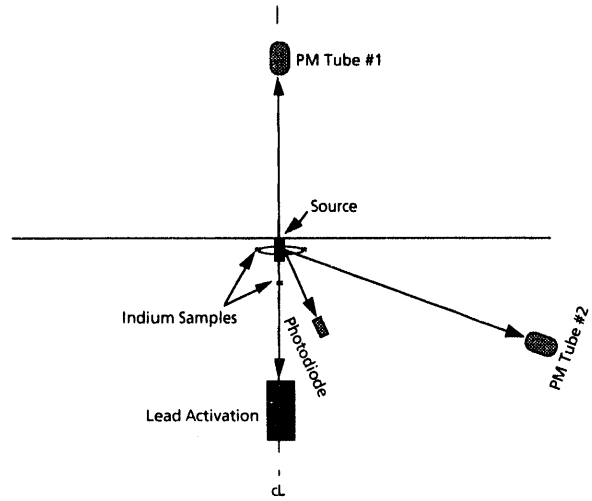

Figure 2 A schematic of the neutron diagnostics fielded on Saturn for the D-D fusion experiments showing their relative orientation. The figure indicates the relative orientation of the neutron diagnostics.

the z-pinch load. Four of the indium samples were 14.5 cm from the pinch axis and one was placed 21.3 cm from the pinch along the axis. The indium was excited to a metastable state via

$$^{115}\mathrm{In}(n,n')^{115m}\mathrm{In}.$$

The metastable state of the indium has a half life of 4.49 hr and the decay gamma ray has an energy of 336 keV. This indium activation technique gives a very accurate determination of the neutron yield. The activated indium samples were read with a 100-cm^3 Ge detector (1.9-keV resolution) immediately following the shot to obtain the initial activity. Overall experimental accuracy is better than $\pm$20%. Absolute calibration of the indium detector system has been reported elsewhere.[8]

We also used a scintillator/photomultiplier (PM) tube diagnostic to measure the time-of-flight history of the neutron pulse. We attempted to look at neutron anisotropy by placing the PM tubes both on and off the axis of the z pinch. We placed the detectors radially (70° off axis) 1.48 m from the source and axially 11.25 m from the source. The distance from the source was chosen to eliminate signal saturation and to get the largest off-axis angle possible. The scintillator/PM was capable of determining the mean energy of the neutrons to $\pm$0.2 MeV. Data from the PM tubes was recorded on 350-MHz digitizers to ensure adequate time resolution. A schematic of the detector arrangement is shown in Fig. 3. The photomultiplier tube was a XP-2020. The extreme sensitivity of this diagnostic to all radiation required us to shield the PM tube with > 15 cm of lead to prevent the hard x-ray background from dominating the signal. The effect of neutron transport in a massive lead shield has been experimentally investigated in Ref. 9. In this work, for D-D neutrons the main effect of the Pb shielding (up to 20.3-cm thick) was to attenuate and broaden the neutron pulse. The rise time of the pulse was found to be relatively unaffected by the Pb shield.

A scintillator/photodiode diagnostic was fielded close to the pinch in order to more accurately measure the rise time of the neutron pulse. By being as close as possible we minimize both neutron scattering and velocity dispersion. Lead shielding was used to minimize the x-ray signal of the diagnostic. (See Fig. 4.)

A lead activation diagnostic was used to measure the absolute neutron yield from the pinch.[10] A schematic of the diagnostic is shown in Fig. 5. The diagnostic was fielded on axis at a distance of 3 m from pinch center. Lead activation has long been used to make total neutron yield measurements of pulsed D-T neutron sources.[11] The technique has been less often employed in the measurement of pulsed D-D sources because of the technique's much lower sensitivity to 2.45-MeV D-D neutrons.[12] For D-D total yield measurements, the diagnostic uses the inelastic reaction $^{207}Pb(n,n')^{207m}Pb$ which has a threshold of 1.6 MeV. This high neutron energy threshold insures complete insensitivity to thermal neutrons and relative insensitivity to other scattered neutrons. Gamma-rays from the decay of the ^{207m}Pb state are counted with a plastic scintillator combination shown. The ^{207m}Pb state has a half-life of 0.796 s. To extend the dynamic range of the technique, NIM fast-logic electronics was used instead of the conventional preamp/amplifier NIM slow-logic counting electronics described in Ref. 10. We used 0.7-1.2-s delays from the prompt radiation pulse and counting intervals of 1.2-2.0 s in an effort to insure that the intense x-ray bremsstrahlung-induced photomultiplier tube noise had decayed to a level near background before counting the ^{207m}Pb signal. Background tests with a reference source showed that accurate measurements could be made with these delays. This set of delays and counting periods enabled the technique to yield data in < 3 s after a shot. The technique was cross-calibrated with the

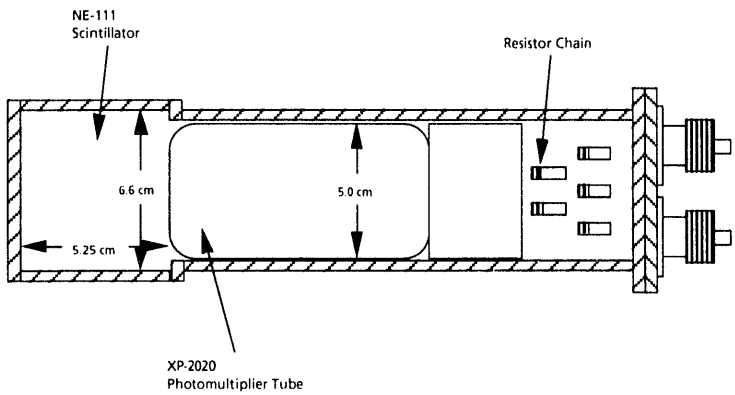

Figure 3 A schematic of Sandia scintillator/photomultiplier diagnostic used for the Saturn experiments. The sensitivity of this diagnostic to hard x rays required large amounts of lead shielding to remove the x-ray background.

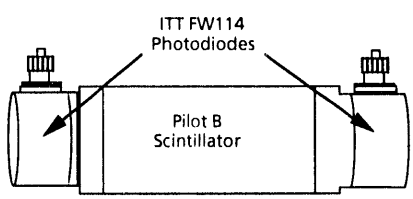

Figure 4 A schematic of the scintillator/photodiode neutron diagnostic showing the two channels, the signal channel and a background channel.

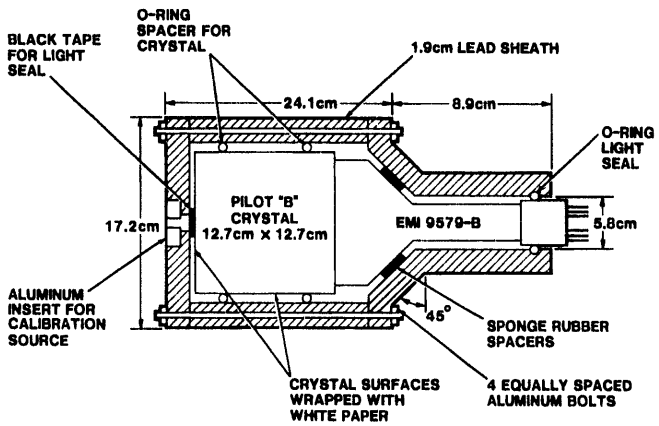

Figure 5 A schematic of the scintillator/photomultiplier neutron diagnostic showing detector geometry, shielding, and electrical connections.

$^{115}In(n,n')^{115m}In$ activation diagnostic described above. System sensitivity was maintained by counting gamma-ray emission of a ^{133}Ba reference source.

DATA

We have plotted the neutron yields from the D-D shots in Fig. 6. The plot shows all of the absolute neutron yields from the indium activation diagnostic. Also plotted is scaled data from the scintillator/PM tube diagnostic. The plot shows data from deuterium gas-puff experiments with a 2.5-cm diameter nozzle, deuterium gas-puff experiments with a 3.5-cm diameter nozzle, and deuterium gas-puff implosions onto a single CD_2 fiber. We were able to obtain D-D neutron yields as large as $3X10^{12}$ on Saturn. The data show an interesting trend. The neutron yields for the shots with a 2.5-cm diameter nozzle first increase with decreasing gas pressure (decreasing pinch mass and increasing pinch temperature) and, then, decrease. We also plot the signal from a gallium-arsenide PCD, filtered with 254 μm of Kapton. This detector looks at x rays above 3 keV. In a hydrogen plasma the x rays are emitted via free-free bremsstrahlung and are indicative of the plasma temperature. A PCD signal from shot 1018 is shown in Fig. 7. The peak signal amplitude of ~ 1.1 V is 2X larger than the signal from shot 1020, which had a mass 25% larger, and is > 5X larger than shot 1023 that had a pinch mass 50% larger. This is very suggestive of a plasma with an increasing electron temperature with decreasing mass. The electron temperature of the deuterium pinch is directly related to the implosion velocity. We measured implosion times (time from the start of the current pulse to the beginning of the x-ray pulse) of 60 to 75 ns. This implies (See the Theory Section.) a specific energy per ion of 3.8-5.2 keV.

In addition to the absolute neutron yield, the indium activation detector provided data concerning the emission isotropy of the source. The four horizontally-mounted and one axially-mounted indium diagnostic gave identical neutron yields, to within the detector accuracy of ±28%, for all of the shots taken on Saturn. These data are remarkably different than the bulk of data from DPF devices. In these machines, it is often claimed that intense, high energy deuterium beams (E > 50 keV) propagating though the pinch plasma are responsible for the observed strongly anisotropic neutron output. In these cases axial neutron emission can exceed radial emission by 5-10X.[13]

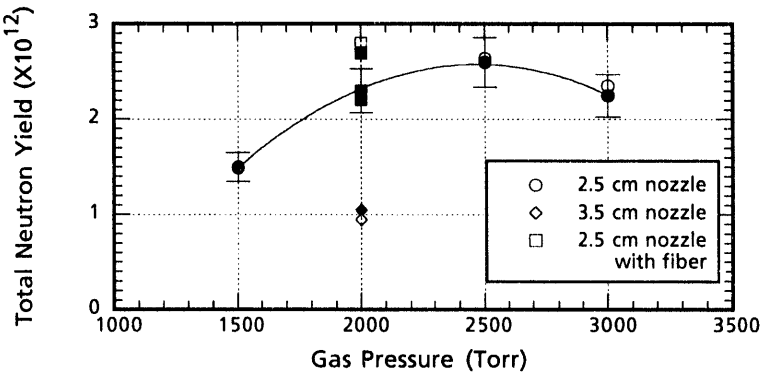

Figure 6 Data from the D-D neutron shots on Saturn for the different plasma conditions of the experiments. Solid points are scaled PM tube data while open circles are yields from the indium activation detector.

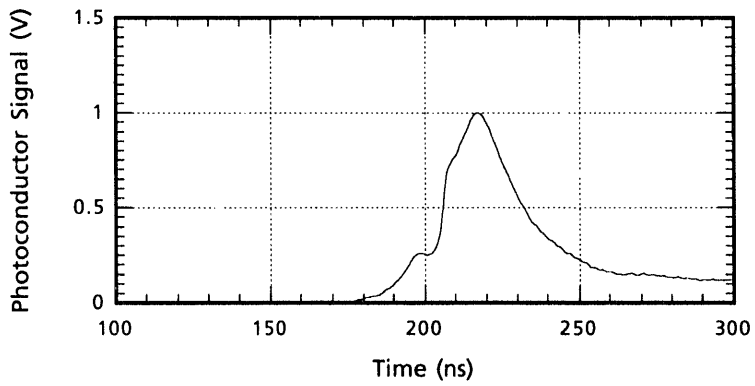

Figure 7 The signal form a gallium-arsenide PCD filtered with 254 μm of Kapton. The signal amplitude is related directly to the electron temperature.

The scintillator/PM tube data quickly confirmed the source of the neutrons by measuring the energy of the neutrons to be 2.45±.2 MeV. The data show the delay due to the velocity of the neutrons, the scattering of the neutrons from the walls and floor of the facility, and, relatively, the neutron output from each shot. It is a simple matter to time reference the neutron signal to the x-ray noise caused by the losses in the power feeds in the high voltage section of the machine. Fig. 8 shows typical data form the scintillator/PM diagnostic.

The rise time of the neutron pulse from the scintillator/photodiode detector was ~ 15 ns implying a burn time of 15-20 ns FWHM (See Fig. 9). This data shows the temporal separation between the hard x-ray background pulse and the neutron pulse. The reduction in the neutron background after the pulse is due to the detectors close proximity to the source.

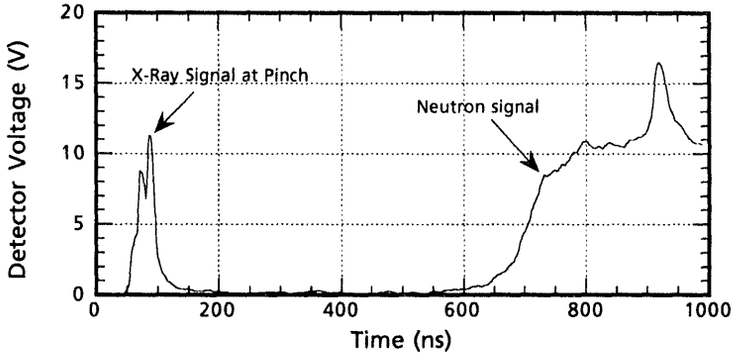

Figure 8 The signal form the scintillator/Photomultiplier tube diagnostic on Saturn Shot 1020 showing a hard x-ray signal at pinch time, the neutron-generated signal, and the late time scatter from the walls.

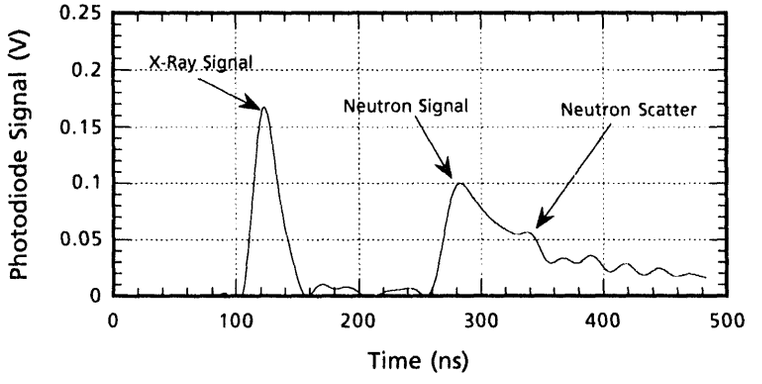

Figure 9 The signal form the photodiode on Saturn Shot 1020 showing a hard x-ray signal the neutron-generated signal and the late time scatter from the near by hardware.

A summary of the data shows that the highest yields were obtained with deuterium gas puff implosions using the 2.5-cm diameter nozzle. A 250-μm-diameter CD_2 fiber on axis gave yields somewhat higher than identical shots without the fiber (Saturn shot 1022). Shots that imploded arrays of CD_2 fibers gave yields several orders of magnitude lower than the gas puff shots. Neutron production was isotropic and was not peaked at plasma conditions consistent with the highest plasma temperature.

One of the indications that neutron output was large was the significant level of neutron activation found in the load region. We found that the most important activation path was neutron activation of aluminum.

$^{27}Al\ (n,\gamma)^{28}Al$, beta decay with a 2.3-m half life

$^{27}Al\ (n,p)^{27}Mg$, beta decay with a 9.5-m half life

We were able to measure the decay of the activation products with both hand-held Geiger counters and the lead activation detector. The activation of the aluminum diode hardware raised personnel health concerns. Outside the vacuum chamber we measured an initial activation level of 100 mR/hr. This required careful measures when recovering the indium activation samples and forced us to wait overnight before handling the power feed hardware.

THEORY

Fusion reaction rates are determined by both the plasma temperature and the plasma density. These values are not independent in z-pinch systems. For a given accelerator there is a range of densities and temperatures that are obtainable. Larger, higher current, drivers can hold the temperatures nearly constant while the peak density increases roughly as I^2. The effective D-D fusion thresholds are set by the plasma temperature through the fusion cross section. Once a temperature > 1-2 keV is reached the number of fusion reactions is most strongly affected by the peak plasma density. For a typical implosion velocity of 70 cm/μs, the radially-directed kinetic energy per deuterium ion is 5.2 keV and the equipartition of that energy between an ion and an electron results in a lossless peak temperature estimate of 1.8 keV. Fig. 10 shows the relation between the implosion time and the implosion velocity for 3.5- and 4.5-cm outer diameter nozzles. These results were obtained with the '0-dimensional' circuit code "ZORK"[14] that used the open circuit Saturn voltage waveform, characteristic circuit parameters of the Saturn accelerator, and the load parameters. No detailed stagnation or radiation physics was included. We used the two different nozzle diameters to reach different implosion velocities and temperatures at varying plasma densities. The plotted implosion times and velocities are representative of these measured in these experiments. Typical deuterium masses were in the range of 0.5-1.0 mg.

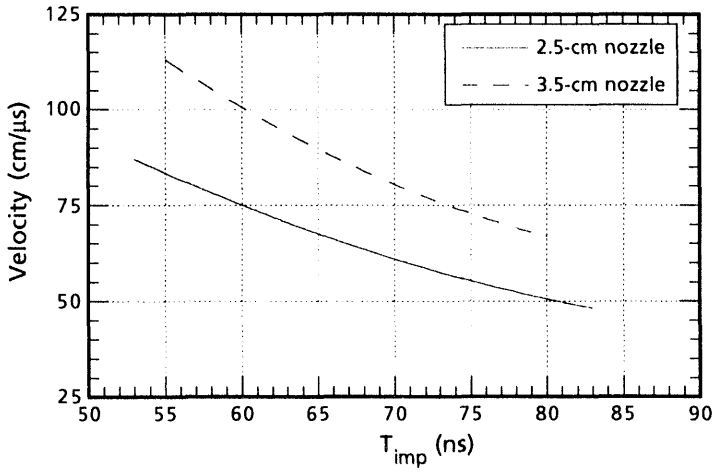

Figure 10 A plot of the peak implosion velocity as a function of the implosion time. These values were calculated using a 0-dimensional circuit code with the Saturn parameters.

The details of the z-pinch implosion and stagnation event are not simple. In these experiments current is applied to an annular deuterium shell. The current is effectively excluded from the interior of the plasma by the plasma conductivity.[15] As the current

increases the magnetic forces begin to implode the plasma shell, snow plowing the interior plasma. Compression and shock heating serve to increase the temperature of the plasma, further increasing its conductivity. As the implosion proceeds the annular shell accelerates and becomes susceptible to the magneto-Rayleigh Taylor instability. The magnitude of this instability is determined by the magnitude of the acceleration and the initial geometry of the gas-puff z pinch.[16-18] As the plasma begins to stagnate the deuterium ions oscillate between the ambipolar fields of the accelerating sheaths because the ion collisionality is too small to thermalize the ions initially. As the pinch density increases the ion-ion collisions increase and the plasma begins to thermalize. At peak compression the density and temperature are maximized. Because of the plasma inertia the density and temperature can temporarily exceed the Bennett equilibrium. During the final implosion and stagnation the pinch may have a plasma resistivity greater than that predicted by Spitzer.[19] We examined the potential role of resistive heating in increasing the pinch temperature. Spitzer resistivity is 2-3 orders of magnitude too low to be significant. Even an increase of 10X in plasma resistivity would not be enough to impact the final pinch temperature. All of these issues need to be addressed in detail in order to obtain a real understanding of the implosion and stagnation. In this paper, we will confine ourselves to simple hydrodynamics modeling described below.

We have used a 1-D MHD computer code to model the implosion. The code, LASNEX,[20-21] included the effects of radiation losses, and kinetic and ohmic heating. LASNEX is coupled to a circuit model of the driver similar to the ZORK code. We found that 1-D MHD codes can be manipulated to achieve any neutron yield desired because the final pinch radius will approach zero when the physical code parameters are set at classical values. By adjusting parameters such as the artificial viscosity and resistivity the final pinch radius and, hence, the density can be limited. In addition, the low level of ion-ion collisionality mentioned earlier means that the assumption of fluid behavior (assumed in an MHD code) is violated. Because of these difficulties we have applied analytic techniques to the data to gain understanding.

From the fact that the neutron yield was measured to be isotropic we conclude that a significant fraction of this yield was thermal rather than beam-target. The thermally averaged D-D reaction cross section as a function of ion temperature, T (keV) is,[22]

$$(\overline{\sigma v})_{DD} = 2.33x10^{14} T^{-2/3} \exp\left(-18.76T^{-1/3}\right) cm^3 / \sec , \qquad (1)$$

which leads to a neutron yield, Y, of

$$Y = 0.5 N n_D (\overline{\sigma v})_{DD} \Delta t \qquad (2)$$

where N is the number of deuterons, n_D is their density, Δt is the time during which the plasma remains assembled, and the factor of 0.5 approximately accounts for the branching ratio. The above expression for yield is a strong function of both temperature and density. It is somewhat surprising, therefore, that the experimentally observed neutron yield should have been relatively insensitive to a wide variation of initial implosion conditions, given that it is well known that density and temperature at pinch depend so strongly upon these initial conditions.[23]

To better understand the processes leading to this apparent anomaly we plot, in Fig. 11, contours of constant neutron yield in pinch radius - pinch temperature space in which we assume that pinch mass per unit length is held constant at 100 μg/cm and that the pinch assembly time is 10 ns. This representation of yield is only approximate because both pinch mass and pinch assembly time are, in reality, variables related to pinch radius and temperature. Nevertheless, these parameters should vary by no more than a factor of a few for implosions that are reasonably efficiently coupled to the electrical characteristics of the Saturn accelerator. Therefore, the trends represented by the curves in Fig. 11 should be qualitatively accurate. We observe that a thermal neutron yield of ~ 10^{12} can be obtained from a cold, tightly pinched region (r ~ 0.10 mm; T ~ 900 eV) or from a much hotter, more

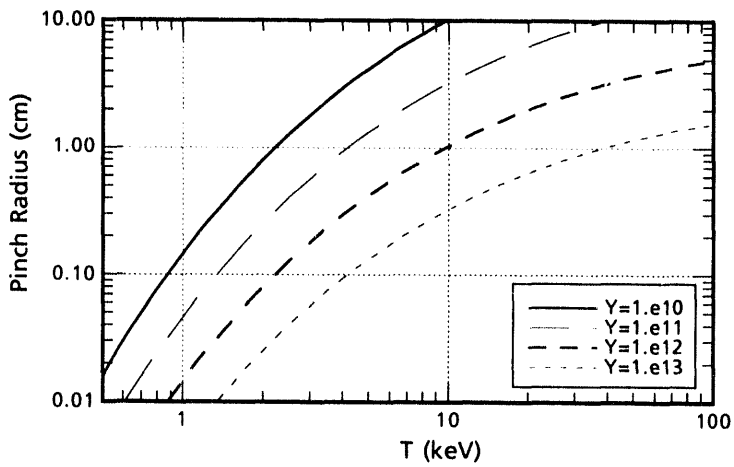

Figure 11 A plot showing the relationship between the final pinch radius, plasma temperature and the neutron yield..

diffuse pinch (r ~ 1.0 cm; T ~ 10 keV). We conclude that experimental variations in pinch initial conditions that were made with the purpose of increasing pinch temperature must also have made the pinch more diffuse.

This observed correlation of pinch density with pinch temperature is not surprising. The pressure of a dynamic pinch is approximately given by rv^2 where r is the density just prior to stagnation and v is the final implosion velocity. Radiation losses from an assembling pinch cool it, but do not greatly modify its stagnation pressure, so that it becomes more dense. Thus, it is possible to increase pinch density, but only at the price of decreasing its temperature, so that neutron yield might be little affected. Therefore, we conclude that to significantly increase neutron yield one must increase rv^2 prior to stagnation. This is also somewhat more difficult than it might seem. To increase the implosion velocity for a given current waveform either one must increase the initial radius (r) with constant mr^2 (decreasing m = mass/length), such that the implosion time remains approximately constant, or one must decrease the mass holding the radius constant, thus decreasing the implosion time.[14] Either case leads to decreased pinch mass per unit length. Furthermore, it is well known that increased implosion velocity leads to increased susceptibility to the hydromagnetic Rayleigh-Taylor instability.[16-18] The non-linear phase of this instability, which is readily achieved by implosions with these parameters, has the effect of thickening the plasma shell during the implosion, thereby decreasing its density just prior to stagnation. Thus, instabilities act to prevent the significant increase of rv^2.

Finally, we have considered more complicated pinch systems designed to increase pinch density sufficiently to more than offset the corresponding decrease in temperature. We considered an on-axis CD fiber to raise the adiabat of the pinch, and we mixed a small amount of high-Z gas with the deuterium in hopes that radiation trapping would keep the core of a pinch sufficiently hot so that the increased density might not be totally offset by cooling. Even these drastic variations in pinch conditions, however, led to little variation in neutron yield, leading one to postulate that significantly increased D-D yield can only be obtained with increased driver power and energy.

CONCLUSION

Deuterium gas-puff z pinches were used to produce up to $3X10^{12}$ D-D neutrons. The isotropy of the neutron emission is indicative of a thermal production mechanism rather than a beam-target process. Our data suggests strongly that plasma density, not temperature, limits fusion reaction rates in our z pinches. Larger drivers or more sophisticated load configurations on Saturn, giving higher final pinch densities, could dramatically increase fusion output. The use of D-T reactions could increase the total neutron yield to $3X10^{14}$. This level of fusion reactions makes Saturn comparable to any existing inertial confinement fusion systems at much lower levels of stored energy.

The use of cryogenic deuterium fibers on the pinch axis should allow much higher plasma densities to be reached in the core of the pinch and result in an increase in the fusion yield. Magnetic field stabilization may also assist in the production of higher density, stable pinches.

REFERENCES

1. D. D. Bloomquist, R. W. Stinnett, D. H. McDaniel, J. R. Lee, A. W. Sharpe, J. A. Halbleib, L. G. Schlitt, P. W. Spence, and P. Corcoran, Proc. of the Sixth IEEE Pulsed Power Conference, Arlington, VA edited by P. J. Turchi and B. H. Bernstein (IEEE, New York, 1987), p. 310.
2. R. B. Spielman, P. Corcoran, J. Fockler, H. Kishi, and P. W. Spence, Proc. of the 7th IEEE Pulsed Power Conf.., (June 1989), p. 445.
3. P. Corcoran, J. Fockler, K. Nielsen, I. Smith, P. Spence, R. B. Spielman, and D. H. McDaniel, Proc. of the Defense Nuclear Agency Advanced Pulsed Power Conference, Albuquerque, NM, (July 1990) p. 32.
4. T. W. Hussey, M. K. Matzen, and N. F. Roderick, J. Appl. Phys. **59**, 2677 (1986).
5. R. B. Spielman, R. J. Dukart, D. L. Hanson, B. A. Hammel, W. W. Hsing, M. K. Matzen, and J. L. Porter, Proc. of the 2nd. Int. Conf. on Dense Z-Pinches, AIP Conf. Proc. **#195**, 3 (April, 1989).
6. R. B. Spielman, Rev. Sci. Instrum. **63**, 5056 (1992).
7. D. L. Hanson, R. B. Spielman and J. P. Anthes, Bull. Am. Phys. Soc. **26**, 910 (1981) and L. P. Mix, E. J. T. Burns, D. L. Fehl, D. L. Hanson and D. J. Johnson, Proc. of the Conf. on Low Energy X-ray Diag., Monterey, CA, AIP NY **75**, 25 (1981).
8. C. L. Ruiz, R. J. Leeper, F. A. Schmidlapp, G. Cooper, D. J. Malbrough, Rev. Sci. Instrum. **63**, 4889 (1992).
9. R. J. Leeper and J. Chang, IEEE Trans. on Nucl. Sci. **NS-29**, 798 (1982).
10. R. J. Leeper, J. L. Porter, D. E. Hebron, G. Cooper, and C. Ruiz, Bull. of Am. Phys. Soc. **34**, 2108 (1989).
11. C. E. Spencer and E. L. Jacobs, IEEE Trans. on Nucl. Sci. **NS-12**, 407 (1965).
12. L. Ruby and J. B. Rechen, Nucl. Instr. and Meth. **53**, 290 (1967).
13. R. Miklaszewski, Fourth Int. Conf. on Plasma Focus and Z Pinches, Warsaw, September 1985, p. 209.
14. M. J. Clauser, L. Baker, D. H. McDaniel, R. W. Stinnett, and A. J. Toepfer, Magnetic Implosion of Plasmas with Short Pulse, High Power Generators, Sandia Report, SAND78-1387C.
15. N. F. Roderick, J. Appl. Phys. **60**, 1269 (1986).
16. N. F. Roderick and T. W. Hussey, J. Appl. Phys. **56**, 1387 (1984).
17. T. W. Hussey, N. F. Roderick and D. A. Kloc, J. Appl. Phys. **51**, 1452 (1980).
18. N. F. Roderick and T. W. Hussey, J. Appl. Phys. **59**, 662 (1986).
19. A. A. Galev and R. Z. Sagdeev, Basic Plasma Physics, A. A. Galeev and R. N. Sudan (eds.), North-Holland, Amsterdam 1984.
20. G. B. Zimmerman, LLNL Report UCRL-748111 (1973).
21. P. D. Nielsen and G. B. Zimmerman, LLNL Report UCRL-53123 (1981).
22. S. Glasstone and R. H. Lovberg, *Controlled Thermonuclear Reactions*, (Van Nostrand, New York, 1960).
23. C. Deeney, P. D. LePell, F. L. Cochran, M. C. Coulter, K. G. Whitney, and J. Davis, Phys Fluids B **5**, 992 (1993).

DATE
FILMED
5/31/94
END